Extended Intravitreal Rabbit Eye Residence of Nanoparticles Conjugated With Cationic Arginine Peptides for Intraocular Drug Delivery: In Vivo Imaging

Ignacio Melgar-Asensio,[1,2] Irawati Kandela,[1] Fraser Aird,[1] Soesiawati R. Darjatmoko,[3] Cristobal de los Rios,[2] Christine M. Sorenson,[4] Daniel M. Albert,[5] Nader Sheibani,[3] and Jack Henkin[1]

[1]Center for Developmental Therapeutics, Northwestern University, Evanston, Illinois, United States
[2]Instituto Teófilo Hernando, Departamento de Farmacología y Terapéutica, Facultad de Medicina, Universidad Autónoma de Madrid, Madrid, Spain
[3]Departments of Ophthalmology and Visual Sciences, Biomedical Engineering, and Cell and Regenerative Biology, University of Wisconsin School of Medicine and Public Health, Madison, Wisconsin, United States
[4]Department of Pediatrics, University of Wisconsin School of Medicine and Public Health, Madison, Wisconsin, United States
[5]Department of Ophthalmology, Casey Eye Institute, Oregon Health Sciences University, Portland, Oregon, United States

Correspondence: Jack Henkin, Center for Developmental Therapeutics, Northwestern University, Silverman Hall room 1587, 2170 Campus Drive, Evanston, IL 60208, USA; j-henkin@northwestern.edu.

Submitted: February 12, 2018
Accepted: July 6, 2018

Citation: Melgar-Asensio I, Kandela I, Aird F, et al. Extended intravitreal rabbit eye residence of nanoparticles conjugated with cationic arginine peptides for intraocular drug delivery: in vivo imaging. *Invest Ophthalmol Vis Sci*. 2018;59:4071–4081. https://doi.org/10.1167/iovs.18-24087

Purpose. Drug delivery by intravitreal injection remains problematic, small agents and macromolecules both clearing rapidly. Typical carriers use microparticles (>2 μm), with size-related liabilities, to slow diffusion. We recently described cationic nanoparticles (NP) where conjugated Arg peptides prolonged residence in rat eyes, through ionic interaction with vitreal poly-anions. Here we extended this strategy to in vivo tracking of NP-conjugate (NPC) clearance from rabbit eyes. Relating $t_{1/2}$ to zeta potential, and varied dose, we estimated the limits of this charge-based delivery system.

Methods. NPC carried covalently attached PEG_8-2Arg or PEG_8-3Arg pentapeptides, having known sequences from human eye proteins. Peptides were conjugated (61–64 per NPC); each NP/NPC also carried a cyanine7 tag (<0.5 dye/particle). In vivo imaging system (IVIS), after intravitreal injection, estimated NPC loss by 800-nm photon emission (745-nm excitation) at 1 to 3-week intervals following initial scan at day 10.

Results. NPC of 2Arg-peptides or 3Arg-peptides showed clearance $t_{1/2}$ of 7 days and 17 days respectively, unconjugated NP $t_{1/2}$ was <<5 days. Doses of 90, 180, and 360 μg of PEG_8-2Arg NPC were compared. The lower doses showed dose-proportional day-10 concentration, and similar clearance. Higher early loss was seen with a 360-μg dose, exceeding rabbit vitreal binding capacity. No inflammation was observed.

Conclusions. This type of cationic NPC can safely increase residence $t_{1/2}$ in a 1 to 3-week range, with dose <100 μg per mL vitreous. Human drug load may then range from 10 to 100 μg/eye, usefulness depending on individual drug potency and release rate, superimposed on extended intravitreal residence.

Keywords: nanoparticles, intravitreal drug delivery, cationic peptides, hyaluronic acid, rabbit eye imaging

Retinopathies and posterior eye diseases affect millions of patients and are major causes of blindness worldwide.[1–3] While new biologics offer improvement, their delivery by repeated intravitreal (IVT) injection is burdensome. Treatment of glaucoma and inflammatory eye disease with small molecules is hampered by unreliable intraocular exposure.[4,5] With increasingly common use of IVT injection of proteins to treat retinopathies, such approaches to both large and small agent delivery are more acceptable but clearance varies with disease state,[6] and is often impractical owing to rapid agent removal, via intraocular drainage systems.[3] IVT clearance survey of over 40 agents in rabbits found most small molecules moving rapidly to the posterior segment, exiting the eye with half-lives from 2 to 24 hours[7] (average near 7 hours), size and H-bonding groups modestly slowing loss. Molecules from 1000 to 3000 MW move more slowly toward retina, with a greater percentage removed via trabecular drainage. VEGF-binding proteins display IVT $t_{1/2}$ of 2 to 3 days in rabbits,[7] 5 to 8 days in patients[8] often requiring re-injection at 4 to 8-week intervals, a frequency causing discomfort and risk of morbidity.[9] Thus, longer IVT residence is actively sought through new biomaterials and devices.[10]

While vitreal viscosity varies according to age and other factors, mesh size of vitreous is estimated from 500 to 1000 nm.[11] Thus, neutral or negatively charged particles <200 nm in diameter move freely, but a strong diffusional slowing is observed above 500 nm. Typical carriers are microparticles (MP), diameters >2 μm, for slow vitreal diffusion. These range over liposomes and micelles, polymers, and thermal gels, for prolonged delivery of agents. MP generally biodegrade for eventual removal, but cannot be sterile-filtered or autoclaved. Their breakdown produces a continuum of sizes, some of which may obstruct the trabecular meshwork (TM), or activate

its phagocytes. Commonly used poly(lactic-co-glycolic) MP (PLGA), though well tolerated in nonocular sites, elicited a foreign body response in rabbit eyes[12]; such MP have recently led to rabbit eye inflammation, and more severe reaction in primates with potential for damage to critical structures.[13] With risk of causing glaucoma or tissue damage, few size-based carriers are approved for nonsteroid drugs, making long-acting, smaller NP (<100 nm diameter) desirable.

Albumin, modified chemically to a polycationic form showed strong slowing of diffusion in vitreous.[14] Later, 200-nm polystyrene particles had 1000-fold slowing of vitreal diffusion when coated with amino groups,[15] presumably via hyaluronate (HA) ionic interactions. Polycationic NP are toxic to cells, one exception being when their positive charge is derived from L-arginine, as first discovered by Zern et al.[16]; noteworthy was that much greater toxicity is observed with D-Arg replacement in otherwise identical particles. This suggests enzymatic detoxification of L-Arg (R), possibly by peptidyl arginine deiminases, when slow diffusion limits cell exposure on the inner ocular surface.

We recently described a NP system based on condensed dextran (CDEX) for extended IVT drug delivery, where small PEG peptides, having 1 to 4 L-Arg per peptide, were stably conjugated to carrier OH groups. Higher Arg per peptide increased NPC zeta-potential,[17] with concomitant slowing of vitreal diffusion, as monitored by rhodamine tag. NPC (approx. 100 kDa, 20–30 peptides/NP) with 4R peptides were highly immobilized, those linked with 2R or 3R peptides gave slow diffusion in freshly isolated rat vitreous, and protamine competition implied an ionic mechanism. These peptide conjugates gave prolonged intraocular residence in rats, histopathology did not find tissue damage. In the present follow-up study, using 2R and 3R peptides, we improved conjugation yield, also enabled continuous in vivo measurement. We evaluate the usefulness and limitations of this delivery system in IVT-injected rabbits. Anchors here are pentapeptides with sequences found in eye proteins, having 2 or 3 R residues, each with Tyr, to detect linkage by UV. We now tag NPC with a long wavelength dye, shown here, in enucleated eyes to give fluorescence emission proportional to dye injected. This enabled intraocular tracking of residual NPC over time by an in vivo imaging system (IVIS) under brief anesthesia. Varied IVT doses of one NPC estimated capacity of this delivery system.

Materials and Methods

Chemicals

Dextran-70, Dextran-10, *p*-nitrophenylchloroformate, *N*-Boc-pyrrolidine-3-carboxylic acid, solvents and chemical reagents were from Sigma-Aldrich Corp. (St. Louis, MO, USA). *N*-Fmoc-amido-PEG_8-carboxylic acid and methoxy-PEG_4amine were from Quanta BioDesign (Plain City, OH, USA). Cyanine7 (Cy7) amine and Cy7 maleimide were from Lumiprobe (Hunt Valley, MD, USA).[18] Thio-peptide: NH_2-Cys-PEG_4-Sar-YN-LYRVRS-NH_2, MW 1,490 g/mol was custom synthesized, via solid state methods by CPC Scientific (Sunnyvale, CA, USA).

Optimization of Anchor Peptides

Our previous studies in isolated vitreous humor and in rat eyes showed that CDEX NP, conjugated with 20 to 30 small amino-PEG (8–12) cationic peptide amides, displayed slow diffusion in vitreous. Peptides with 2, 3, or 4 R per peptide, as their only charged groups, had increased zeta potential, which inversely affected NPC diffusion.[17] Here we focus on 2R and 3R anchor peptide amides, each with just five total amino acids, duplicating natural sequences to minimize immunogenicity. For 2R and 3R peptides, we respectively used the natural sequences: YRVRS-amide from pigment epithelium–derived factor (PEDF, residues 66–70),[19] and RRYRL-amide, a sequence conserved in both Hsp 20 and in A-type α-Crystallin (residues 121–125)[20]; these proteins are all intraocular. Peptide extension from the NP surface was via amino-PEG_8 at the N-terminus of peptide amides. Conjugation to activated CDEX OH groups was enhanced, and yield improved by appending (R, S)-pyrrolidine 3-carboxylic acid on amino-PEG_8. The latter efficiently linked PEG-peptides to the carrier as stable pyrrolidine carbamates.

Synthesis of Anchor Peptides for Conjugation

The N-terminal-capped, pyrrolidine-3-carboxyamido-PEG_8 anchor peptides: pyrrolidine-3-CO-PEG_8-CO-RRYRL-amide. MW: 1281 g/mol, (3R peptide); and pyrrolidine-3-CO-PEG_8-CO-YRVRS-amide. MW: 1198 g/mol, (2R peptide) were synthesized via Fmoc-based solid-state peptide synthesis on rink amide 4-methylbenzhydrylamine resin using a CEM Liberty Blue microwave-assisted peptide synthesizer. Fmoc-N-amido-PEG_8-carboxylic acid addition was carried out by manual coupling, using *N,N,N′,N′*-tetramethyl-*O*-(1*H*-benzotriazol-1-yl) uronium hexafluoro-phosphate (HBTU) and excess *N,N*-diisopropylethylamine. Following the Fmoc removal, *N*-Boc-pyrrolidine-3-carboxylic acid was then coupled using HBTU and excess diisopropylethylamine. After cleavage from the resin and deprotection with trifluoroacetic acid (TFA), the final product peptides were purified by HPLC and lyophilized. Peptide purity before conjugation (>95%) was confirmed by analytical HPLC and mass spectrometry.

Cholesterol Dextran (CDEX) Nanocarriers

CDEX was prepared from 70 kDa Dextran (Dex-70), essentially as described by Li et al.[17] Briefly, the condensed nanocarrier was formed by reaction of 4 g Dex-70 with 4 mol % cholesterol, (based on 365 glycosyl monomers per 70 kDa, 4 g = 21 mmol), attached to polymer hydroxyl groups. Dextran was first dried by twice repeated rotary evaporation from anhydrous pyridine, then high vacuum over P_2O_5. Cholesteryl chloroformate (0.4 g, 0.88 mmol) and one equivalent of triethylamine (TEA) in anhydrous dimethyl sulfoxide (DMSO) formed CDEX.[17] Exhaustively dialyzed product was sonicated to maximize internalization of hydrophobic groups. Cloudy CDEX solution was sequentially filtered through filter paper, then through syringe filters of 0.80 μm, 0.45 μm and 0.20 μm pore size, final filtrate lyophilized. Cholesterol groups self-associate to form a core, in the condensed dextran (CDEX, 75 kDa).

CDEX Activation

1,1′-Carbonyldiimidazole, previously used[17] for CDEX-OH group activation, cannot be sensitively quantified to confirm complete discharge upon reaction with amines. Improved activation here with *p*-nitrophenylchloroformate (*p*-nPCOCl) formed a mixed carbonate between sugar OH groups and *p*-nitrophenol (*p*-nP). The yield of sugar-*p*-nP carbonate is readily quantified for control of this first synthetic step, by reaction of precipitated *p*-nP polymer with aqueous base, and UV assay of intensely yellow *p*-nitrophenolate ion at $\lambda = 401$ nm, ($\varepsilon = 18{,}400\ M^{-1}\ cm^{-1}$).[21] Formation of *p*-nitrophenyl carbonates was additionally demonstrated, in parallel, by H^1-NMR (Avance III 500 MHz system; Bruker, Billerica, MA, USA).

Full discharge of the activating group is likewise ascertained in NPC, dialyzed, and lyophilized, following reaction with

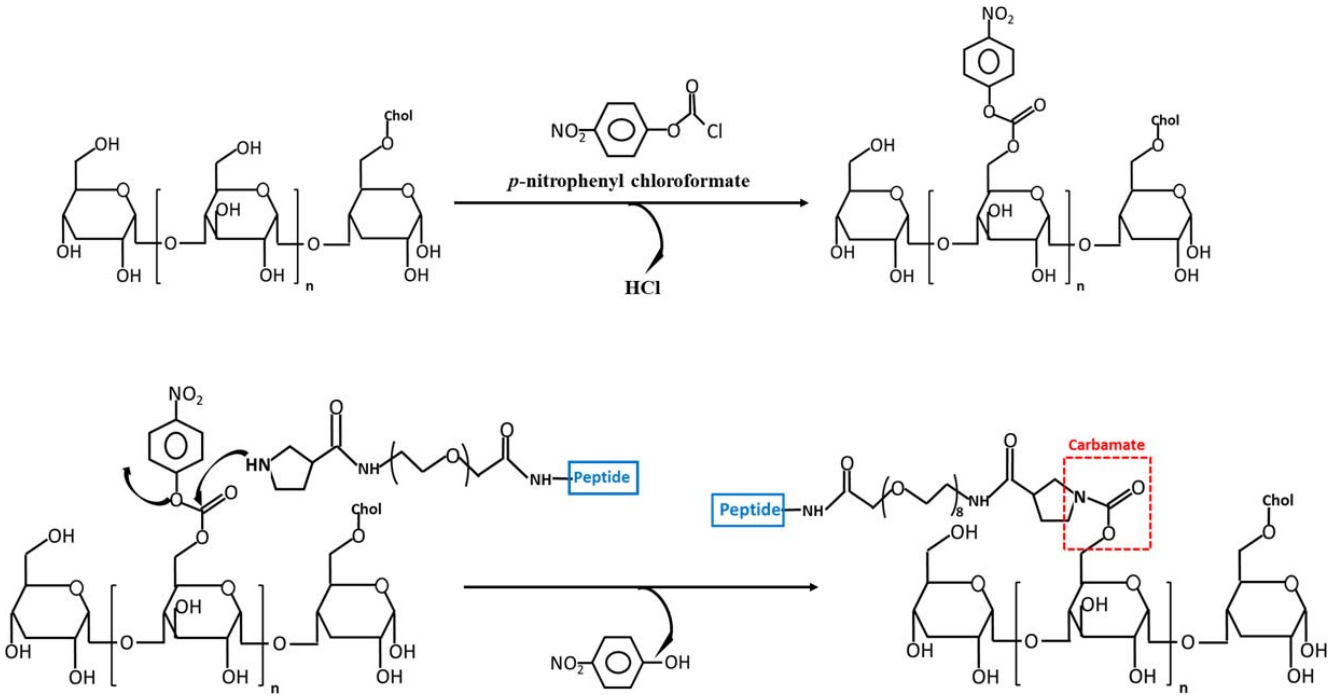

FIGURE 1. Synthetic steps in forming CDEX NPC. CDEX glucosyl-OH groups are activated with *p*-nitrophenyl chloroformate in DMSO/pyridine, polymer then isolated by EtOAc precipitation. Pyrrolidyl-PEG-peptide then displaces *p*-nitrophenol in DMSO to give stable, carbamate-linked peptide. Low stoichiometry Cy7 amine is included during peptide coupling, excess *p*-nP carbonates are then quenched by excess methoxy-PEG_4-amine (not shown).

pyrrolidine-3-carboxamido-PEG peptides, then quenching by excess PEG_4-amine. Final exhaustive aqueous dialysis of NPC, and freeze-drying gave powder, without detectable yellow *p*-nitrophenolate absorbance in aqueous base, <0.01 mol % residual *p*-nP/NP being detectable. Activation and amine coupling steps are shown in Figure 1, synthetic detail below.

CDEX was activated for the peptide attachment by *p*-nPCOCl following the methods of Vandoorne,[22] and Ramirez,[23] with minor modifications. Sterile-filtered, lyophilized CDEX NP 3.0 mg (75 kDa, 14 μmoles glycosyl units,) was dissolved in 200 μL of a mixture of dry DMSO and dry pyridine in 1:1 volume ratio. Then, dimethylaminopyridine (DMAP) catalyst was added to a final concentration of 3 mM. We then added 11 mg (54 μmoles, 3.9-fold excess) of solid *p*-nPCOCl to activate CDEX, at −20°C in a sealed tube. After 17 hours, to quantify *p*-nP covalently linked to CDEX, a 5-μL portion was mixed with 1 mL of ethyl acetate (EtOAc). The precipitate was centrifuged, solvent decanted and centrifugation repeated, resuspending with a second 1 mL of EtOAc, supernatant decanted. The pellet, CDEX-$(p\text{-nP})_n$ was then dissolved in 1.0 mL of 0.1 M NaOH, and UV-Vis spectrum scanned in a quartz cuvette (250–600 nm), after 10X further dilution. This gave 0.23 OD at 401 nm, indicating 125 *p*-nP groups per NP, based on *p*-nitrophenolate extinction.[21] The bulk reaction (0.038 μmoles CDEX, 4.75 μmoles *p*-nP groups) was quenched with 2 mL of EtOAc, the white suspension was centrifuged as above, solvent decanted, and pellet washed by recentrifugation with 2 additional mL EtOAc. UV spectrum in aqueous base, again indicated that 1/3 of the sugars were activated. When comparing the ^{1}H NMR spectrum of free *p*-nitrophenol (*p*-nP-OH) at 500 MHz, ([DMSO-d_6] δ 8.18–8.09 [m, 2H], 6.97–6.90 [m, 2H]) with that of the activated product, the latter displayed new resonances, in the aromatic 6 to 9 ppm region, distinct from those of free *p*-nP-OH ([500 MHz, DMSO-d_6] δ 8.26–8.18 [m, 2H], 7.51–7.42, [m, 5H]), indicating new, attached *p*-nitrophenyl groups.

Peptide and Cy7 Conjugation to Form Tagged NP/NPC

The above pellet was dissolved in 200 μL DMSO, transferred to a 4-mL vial and subjected to rotary evaporation under high vacuum. Then, 2.8 μmoles of the pyrrolidine-amido-PEG_8-peptide (TFA salt) was dissolved in 200 μL DMSO with 10.0 μmoles of dry TEA (1 μL, 3.6-fold molar excess) and 0.038 μmoles of Cy7 amine (from 20 mM stock in DMSO). This was added to the DMSO solution of dry CDEX-$(p\text{-nP})_{125}$, the sealed reaction heated at 45°C, with shaking over 6 days. Reaction was then quenched with 20 μmoles of methoxy-PEG_4-amine at RT over 30 minutes. The mixture was added dropwise to 2.5 mL of aqueous 0.2 M HCl, then dialyzed against three 5 L changes of 0.1 mM HCl over 24 hours, sterile filtered and lyophilized. In the case of nonconjugated (CDEX-70-0) control, all steps were carried our as above, except that peptide was omitted, thus all *p*-nP groups were displaced only by PEG-amine and trace Cy7.

Synthesis of LMW Cy7 Test Compounds for Ex Vivo IVIS Calibration

A peptide-linked Cy7 and a dextran-10-linked Cy7 derivative were synthesized to calibrate imaging in enucleated rabbit eyes. The first compound was formed from thio-peptide NH_2-Cys-PEG_4-Sar-YNLYRVRS-NH_2 by reaction with Cy7 maleimide. The peptide (2.9 mg) was dissolved in in 310 μL of 2 mM acetic acid. Free SH content in this solution was estimated by titration of a 10 μL aliquot with 0.1 mM Ellman's reagent, indicating [cysteine-SH] was 5.9 mM. We added 100 μL (0.59 μmoles thio-peptide) of this solution to a mixture of 400 μL 20 mM HEPES (pH 7) and 220 μL acetonitrile. To this was added 40 μL of 10 mM Cy7 maleimide (0.4 μmoles) in DMSO. Reaction progress was monitored by HPLC (C18, water: CH_3CN), showing complete reaction of the maleimide in 15 minutes. The

water-soluble product, sulfide-linked Cy7-thiopeptide (Cy7-mal-S-Cys-PEG$_4$-Sar-YNLYRVRS-amide, MW approximately 2.2 kDa), was isolated by HPLC and concentrated by rotary evaporation and lyophilization.

The second calibration compound (MW 11 kDa) was 10 kDa dextran (Dex-10), conjugated as carbamate to Cy7 amine. For dye labeling, Dex-10 was activated as described for CDEX-70: 5 mg (10 kDa, 30 μmoles glycosyl units) was dissolved in 200 μL dry DMSO: pyridine (1:1), with DMAP at 3 mM. 23 mg (114 μmoles) of solid *p*-nPCOCl was then added to activate Dex-10 at −20°C in a sealed tube. After 17 hours, to quantify *p*-nP covalently linked, a 5-μL portion was centrifuged twice in 1 mL EtOAc. Pellet, Dex-10-(*p*-nP)$_n$ was dissolved in 1.0 mL of 0.1 M NaOH. UV spectrum after 10X further dilution gave 0.24 OD at 401 nm, indicating 11 *p*-nP groups per Dex-10.[21] We subjected 40 μL of the reaction subjected to EtOAc workup, and the pellet (0.1 μmoles Dex-10) was dissolved in 200 μL DMSO, transferred to a 4 mL vial and evaporated under high vacuum. We added 1 μmol of Cy7 amine (50 μL 20 mM stock in DMSO), containing 1 equivalent of TEA, to the DMSO solution of dry Dex-10-(*p*-nP)$_{11}$ and the sealed reaction heated at 45°C, with shaking over 3 days, then quenched with 20 μmol of ethanolamine over 30 minutes. After dropwise addition to 2.5 mL of aqueous 0.2 M HCl, this was dialyzed exhaustively versus 0.1 mM HCl, sterile filtered, and lyophilized. Based on the 750-nm extinction coefficient of Cy7, 0.5 dye molecules were attached per Dex-10.

Imaging Ex Vivo: IVIS Response to Injected Cy7 Compounds in Enucleated Rabbit Eyes

In order to evaluate the total dye dependence of photon emission in the above IVIS scans of rabbit eyes in vivo, we first administered injections of the above Cy7-tags in freshly enucleated eyes from rabbits following euthanasia, after their nonocular use (spinal surgery). Wavelength and field settings, and the circular ring of emitted photon quantitation, with fixed area of 3.51 cm^2 were identical to those used in the in vivo scans described below, under "Imaging In Vivo." We injected 50 μL of Cy7-thio-peptide solution, or 100 μL of aqueous Cy7-Dex-10 at midline, each eye received Cy7 OD (750 nm) ranging from 0.01 to 0.091 (50–450 pmol dye). IVIS scan (745-/800-nm excitation/emission) was carried out on each eye 24 hours after injection, with pupils facing upward, following RT storage in 20 mL PBS, and photon/s emission recorded by IVIS.

In Vivo Clearance of Peptide-Conjugated NPC From Rabbit Vitreous: Rabbit IVT Injection

NP and peptide-NPC samples were dispersed giving a stable, transparent mixture, at 3 mg/mL in 10 mM phosphate buffer with NaCl 100 mM, pH 7.2. These were: CDEX-0, with no peptides and 0.16 dye per NP; CDEX-3R, with 61 peptides and 0.28 dye per NPC; CDEX-2R with 64 peptides and 0.24 dye per NPC. The latter was also prepared at 6 and 12 mg/mL, all samples sterile-filtered.

We injected 9-week old rabbits (1.8 kg, White New Zealand, Charles River Laboratories, Wilmington, MA, USA) to ensure prone fit within the apparatus. All animal experiments were carried out with adherence to the ARVO Statement for the Use of Animals in Ophthalmic and Vision Research. Rabbits were anesthetized by an intramuscular (IM) mixture of ketamine hydrochloride (20–35 mg/kg) and xylazine hydrochloride (3–5 mg/kg), further local anesthesia provided by additional propacaine. Topical antimuscarinic tropicamide (Mydriaticum) was also administered to obtain the mydriasis (pupil dilation) effect. Before injections, eyes were flushed with povidone for prophylactic local antisepsis.

To inject formulations, eyelids were retracted with a pediatric Barraquer wire speculum and the ocular bulbar conjunctiva were grasped at the lateral canthus via forceps to laterally rotate the globes toward the medial canthus. The needles tip, with their bevel directed backward were positioned on the lateral sclera 4 to 5 mm posterior to the limbus. Each eye was replaced to its natural position and a 31-gauge, 8-mm length needle (fixed to BD insulin syringe) was directed backward with an approximate angle of 45° and pushed through the sclera into the posterior ocular chambers toward the center of vitreous, until the needle base just contacted the eye surface. Volumes of 30 μL were injected. Needles were slowly withdrawn after the injections and the scleral conjunctiva were slightly compressed with the forceps tip to avoid any release of the injected material. Lastly, eye ointment was added topically at the end of the procedure. Intramuscular yohimbine (0.2–1 mg/kg) was used to reverse the effects of ketamine and xylazine (1 mL syringe, 25 or 27-gauge needle).

Imaging In Vivo

Prior to imaging, rabbits were anesthetized by IM injection using ketamine/xylazine. Eyes were kept open for the duration of the imaging procedure, which required less than 1 minute, with eyes opened in the IVIS chamber <45 seconds. However, to avoid corneal drying, ophthalmic solution eyewash (Akorn Animal Health, Lake Forest, IL, USA) was added to moisten the eyes before imaging. Fluorescence signal intensity was imaged on an in vivo imaging system (IVIS; Xenogen IVIS Spectrum; Caliper Life), animals were scanned for fluorescent intensity, on left and right sides, the system being set to 745-nm excitation, and 800-nm emission. Field of view for the IVIS scan was a 13 × 13 cm square (169 cm^2) to include the entire rabbit head on one side. Within this field, a circular subfield, surrounding the eye with area of 3.51 cm^2 was selected for photon emission quantitation, reported photons/s are normalized to photons/s/cm^2 within this circle of constant area. The first scan was always at day 10 postinjection to allow IVT distribution, scans were then repeated at time points (1- to 3-week intervals) up to 52 days postinjection. Animals were euthanized between 8 to 9 weeks after IVT injection, under anesthesia, by injection of 100 mg/kg sodium phenobarbital.

Results

NPC Characterization

Figure 2 schematically illustrates the intended NPC, with peptides as anchors, to slow diffusion via multivalent weak ionic interactions with HA. An UV-Vis absorbance spectrum of the 3R-NPC in water at 1.0 mg/mL is shown in Figure 3. A peak at 275 nm, not present in unconjugated NP, is from a single tyrosine in each peptide. The minimum height of this peak, subtracting only the high background scattering at 300 nm, leads to calculation of at least 27 to 30 peptides/NPC, based on Tyr molar extinction of 1100 at 275 nm, a minimum estimate since light scattering goes up sharply and indeterminately at lower wavelength. Correction to the baseline of a spectrum of similarly activated but only methoxy-PEG$_4$-amine quenched CDEX-0, estimates ~60 peptides per NPC but is uncertain as particle size varies. Thus, UV is a crude measure of peptide load. More accurate peptide load determination on weighed samples was accomplished by the same bicinchoninic acid (BCA) colorimetric assay procedure described previously,[17] where standard curves were based on BCA reaction of the free peptides. Cy7 attached to CDEX was quantified by Vis

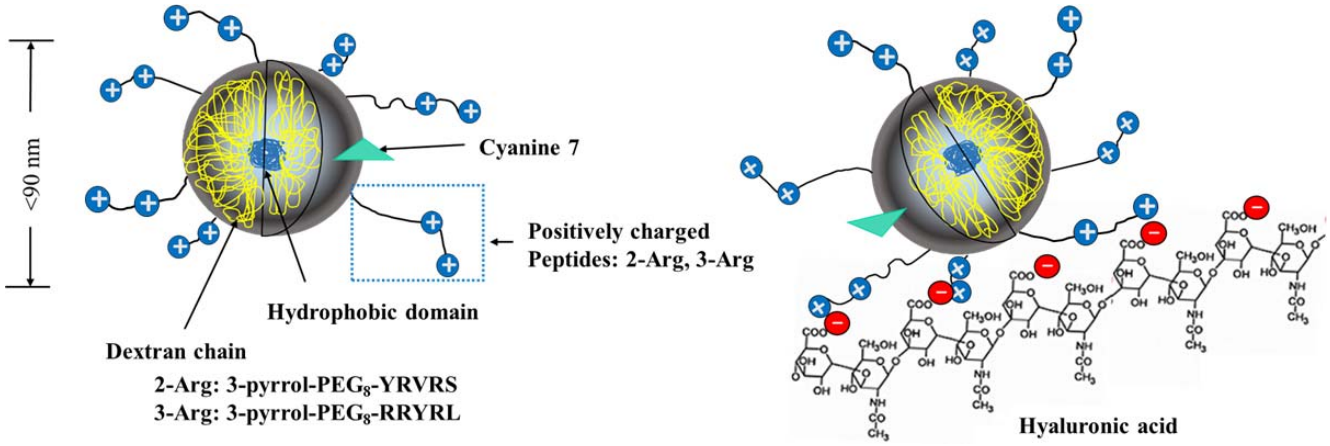

FIGURE 2. Schematic view of CDEX peptide-conjugates (NPC) in vitreous. A hydrophobic cholesteryl domain forms the CDEX NP core. Conjugated PEG-peptides extend outwards. NP are labeled by Cy7 amine, to yield <1 Cy7/NPC. Two types of positively charged peptides were linked at 61 to 64 peptides per NP (lower loading shown for un-crowded view). NPC are immobilized in vitreous by ionic binding between l-Arg guanidinium groups (*blue circles*) on NPC surface and HA polymer (*red circles* are HA carboxylate groups).

spectrum ($\lambda = 750$ nm; $\varepsilon_{Cy7} = 199{,}000\ M^{-1}\ cm^{-1}$)[18] as in Figure 3.

This showed the number of peptides linked per particle for the three nanocarriers (CDEX-0, CDEX-2R, and CDEX-3R) to be 0, 64, and 61 respectively. Thus, the number of positive charges, derived exclusively from Arg residues per NP/NPC were 0, 128 (64 peptides × 2R per peptide) and 183 (61 peptides × 3R per peptide). NP/NPC diameter and zeta potential were measured by dynamic light scattering (DLS) and electrophoretic mobility ($n = 3$) with a Zetasizer Nano ZSP (Malvern Instruments, Malvern, UK). Properties of the NP/NPC are summarized on Table 1.

The measured zeta potential of the conjugates increased with the number of positive charges per particle (CDEX-0: –0.61 ± 0.1 mV, CDEX-2R: 3.9 ± 0.9 mV, CDEX-3R: 6.34 ± 1.3 mV) and particle size was CDEX-0: 150 nm, CDEX-2R: 85 nm, CDEX-3R: 82 nm. Percent CDEX mg recovered was based on the total mg of CDEX used, corrected to the theoretical added masses of peptide and PEG_4-amine. Lower yield in unconjugated CDEX (PEG_4-amine only) may reflect multimeric aggregates lost on sterile-filtration, since NP without peptides are not cationic, thus not self-repelling. These may unfold during dialysis and coalesce via exposed hydrophobic surfaces. Traces of multimeric CDEX NP without peptides may well lead to overestimated size by DLS. We attribute the smaller diameters of cationic conjugates to mutual charge repulsion, and structure stabilization, preventing such self-association. Cy7 OD (750 nm) showed less than 0.3 dye molecules/particle. This low level was sufficient to study the diffusion of tagged NP/NPC in vitreous while unlikely to perturb diffusion, the dye being uncharged and <0.5% of any particle mass (100–160 kDa). Cy7 is a very sensitive and useful tag, we found that it must be protected from degradation by UV or extended room-light exposure.

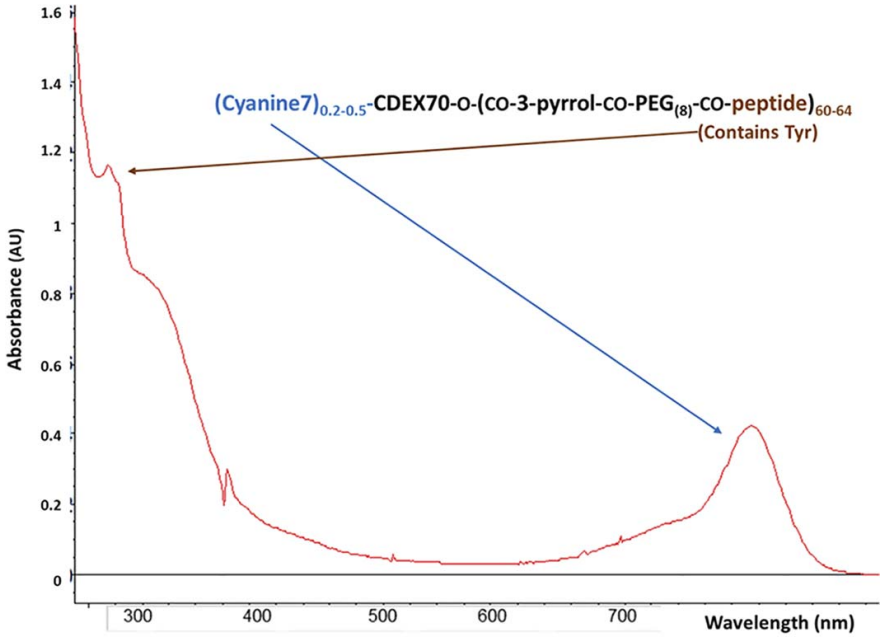

FIGURE 3. UV-VIS spectrum of Cy7-CDEX-3Rpeptide conjugate. λ_{max} of peptide tyrosine: 275 nm, λ_{max} of Cy7: 750 nm. The peak Cy7 molar extinction is 180-fold higher than that of Tyr.

Table 1. Physicochemical Characteristics of NP and NPC

NP or NPC	Pept/CDEX	Positive Charges/CDEX	ζ, mV	Cy7/CDEX	Particle Diameter, nm	% CDEX Mass Recovered
Cy7-CDEX-0	0	0	−0.6 ± 0.1	0.16	150 ± 2	50
Cy7-CDEX-2R	64	128	+3.9 ± 0.9	0.24	85 ± 15	80
Cy7-CDEX-3R	61	183	+6.3 ± 1.3	0.28	82 ± 7	90

ζ, zeta potential.

In Vivo Clearance From Vitreous Is Surface Charge (Zeta Potential)–Dependent

For the in vivo fluorescence-based eye clearance study, the IVIS system generates images according to the flux of photon/s emitted (800 nm) in a defined circular area surrounding the rabbit eye facing upward upon excitation at 745 nm. Each rabbit eye received 30 µL, by IVT injection, of one of the three samples (Cy7-CDEX-0, Cy7-CDEX-2R, Cy7-CDEX-3R) each at 3 mg/mL. After injection, 10 days elapsed before the first IVIS eye imaging to allow NP/NPC distribution, to minimize variation in fluorescent yield caused by sharp early volume change. Most initial fluorescence intensity, in peptide-loaded NPC was retained in the eye during this time period, based on day 3 (not shown) versus day 10 comparison. The loss of the Cy7-tagged particles was followed over up to 6 weeks beyond day 10. The change of fluorescence intensity for exemplary individual rabbit eyes is shown on Figure 4. This illustrates how individual eyes injected with equal amounts of Cy7-tagged NP/NPC can be repeatedly imaged over 1- to 3-week periods for estimation of emitted photons/s, a measure of ocular retention since dye is linked as a stable carbamate (urethane) bond. 3R-NPC were lost from the eye more slowly than 2R-NPC, while unconjugated NP were rapidly lost.

Figure 5 shows emitted photon flux over the eye area, estimated by the IVIS instrumentation at specified times for a single eye, which had received 3R-NPC, then was scanned at different times. Background autofluorescence (preinjection) ranged from 0.8–0.9 × 10^9 photons, the average being 0.82 × 10^9. For tabulated decay analysis, all data were corrected by subtraction of the average autofluorescence background of the eyes obtained before treatment, this was 6- to 8-fold lower than the fluorescence observed at day 10 postinjection. Emitted photon flux measured on day 10 was then taken to be 100% for calculation of percent loss measured on subsequent elapsed days. Thus, in the eye shown, there was an initial signal-to-noise ratio of approx. 7:1, dropping to 2.3:1 after 6 weeks. The percent emitted photons, corrected by subtraction of average autofluorescence flux from all other measured flux values, reached 22% of the original value in this eye at 6 weeks beyond day 10, corresponding to $t_{1/2}$ of 2 weeks in that eye if emission is proportional to NPC.

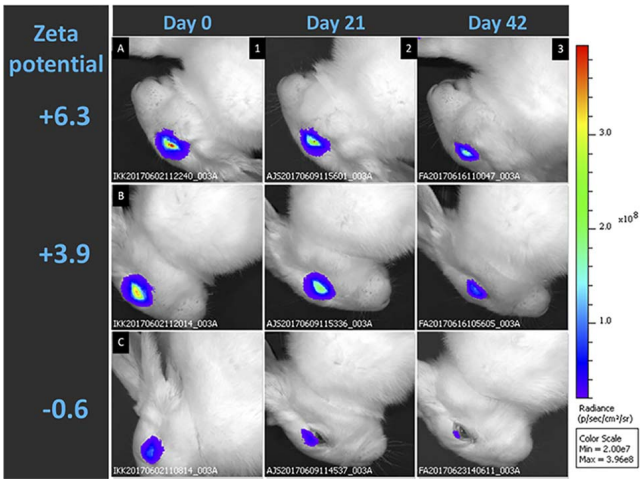

Figure 4. Loss of intraocular NPC over 6 weeks at varied zeta potential. Decay of intraocular fluorescence at 3 and 6 weeks, at and beyond postinjection day 10 ("day 0") is seen in individual eyes injected with Cy7-tagged 3R-NPC (*top row*), 2R-NPC (*middle row*), and unconjugated NP (*bottom row*). Spreading and loss of fluorescence is slowed in more highly charged NPC, with correspondingly greater zeta potential.

IVIS-Detected Fluorescence Response to Cy7 in Enucleated Rabbit Eyes

Three rabbit eyes were enucleated within 4.5 hours of euthanasia (IV Euthasol infusion). The eyes were immersed in cold PBS, then brought to RT and injected, with 50 µL each of 3 varied concentrations of Cy7-thio-peptide (OD 750 nm 0.22–1.8), IVIS scan was then performed on each injected eye after 24 hours immersion at RT in PBS. One week later, eight eyes were enucleated identically and two eyes each were injected with 100 µL each of one of four varied concentrations of Cy7-Dex-10 (OD 0.11–0.67), with IVIS scan again obtained at 24 hours. The results of this calibration between injected Cy7 and photon flux are seen in Figure 6A, with Cy7 concentration and emission detail given in Table 2, showing that over the range of 3.6–31 × 10^9 emitted photons/s from any rabbit eye, the instrument photon count was proportional to the amount of Cy7 injected, giving a constant ratio of photons/s per injected nmol Cy7 (average 66 × 10^9 photons/s per injected nmol; range, 56–76 × 10^9), normalized to 1 cm^2 within the 3.51 cm^2 circle. Background autofluorescence was 1.35 × 10^8 photons/s, always <5% of the photon flux, ~6-fold lower than found in live rabbit eyes. In the test range (ex vivo overlays in vivo range), photon flux is a direct measure of IVT Cy7 concentration.

Estimate of Clearance Half Lives in NP and NPCs

For graphical decay analysis, emitted photon/s were corrected by subtraction of the average autofluorescence background of the eyes obtained before treatment. Emitted photon flux measured on day 10 was then taken to be 100% for calculation of percent loss measured on subsequent elapsed days. Averaged percent decay of fluorescence over time is shown for two imaged eyes injected with unconjugated NP (Figure 6B), and for 3 imaged eyes receiving each conjugate (Figure 6C), details of the emission being given in Table 3. The rate of loss of the three particle types was in the following order: CDEX-0 > CDEX-2R > CDEX-3R. The half-life of CDEX-0 (control) in the vitreous was <3 days, based on loss of fluorescence after day 17 postinjection. While 35% of day 10 photon emission for the unconjugated NP remained at day 17, flux in these eyes approached background by day 24, thus $t_{1/2}$ must be <3 days after day 17. The half-life of CDEX-2R was near 7 days (range, 6–9), at which time, the average remaining

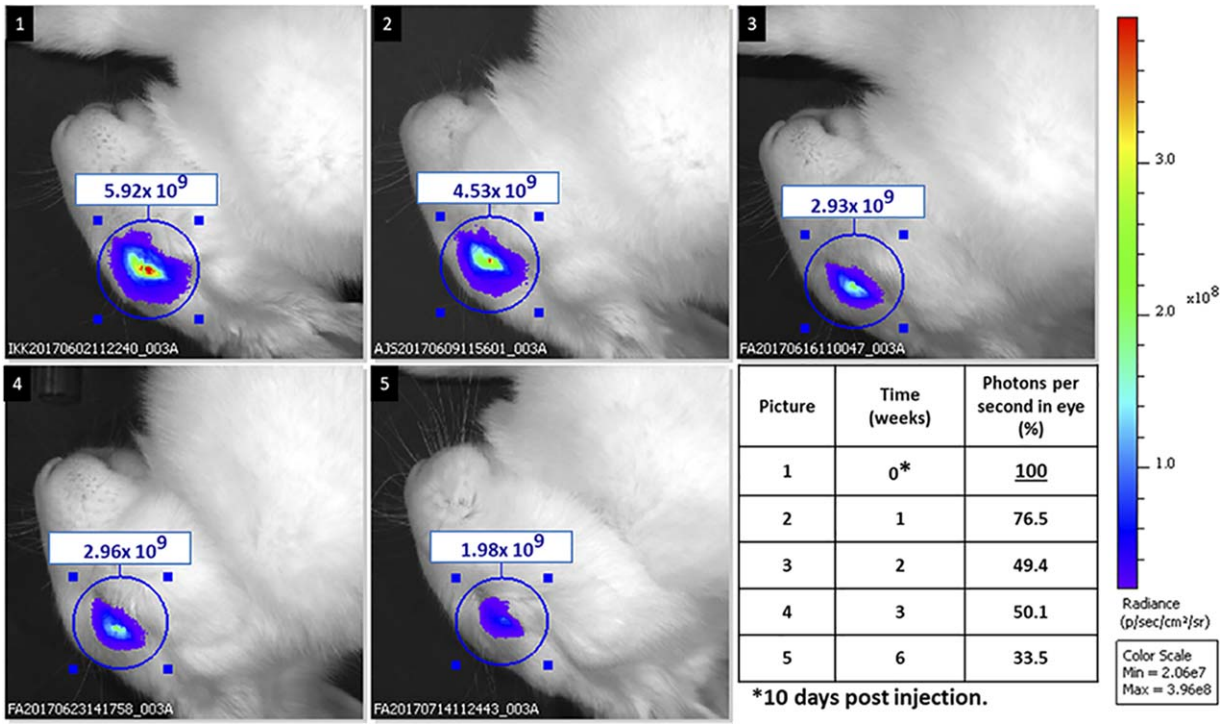

Picture	Time (weeks)	Photons per second in eye (%)
1	0*	100
2	1	76.5
3	2	49.4
4	3	50.1
5	6	33.5

*10 days post injection.

Figure 5. Loss of 3Arg NPC in a single eye over six weeks. A single exemplary eye injected with Cy7 tagged 3R-peptide conjugate is followed by IVIS over 6 weeks beyond the first scan at day 10 postinjection ("day 0"). Photon flux is registered in the rectangle above each eye, designating 800 nm photons emitted per cm^2, within the 3.51 cm^2 circle shown around each eye. Values were corrected by subtracting the autofluorescence (photon emission of eyes before any injection), and percent of "day 0" remaining tabulated. 22% remains after 6 weeks in this eye.

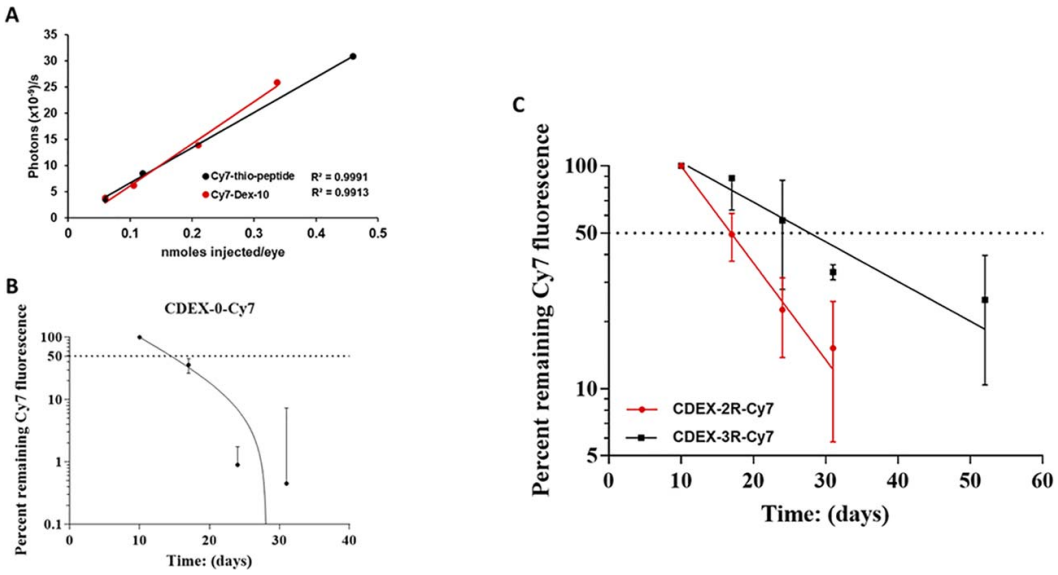

Figure 6. In vivo loss of NP and NPC (2R, and 3R) from rabbit vitreous over time. (**A**) Ex vivo calibration of photon/s emission per cm^2 in 3.51 cm^2 circles surrounding freshly enucleated rabbit eyes injected with specified amounts of Cy7 derivatives, all scans at 24 hours postinjection. *Red line* is 3 concentrations ($n = 1$) of 50 µL injected Cy7-thiopeptide. *Black line* is 4 concentrations ($n = 2$) of 100 µL injected Cy7-Dex-10. Details of these scans are shown on Table 3 and indicate a constant ratio of photon flux to injected nanomoles of Cy7, validating the in vivo pharmacokinetics of Cy7-tagged NP and NPC. Ex vivo autofluorescence was <5% of the lowest Cy7 flux. (**B**) In vivo IVIS scans of Cy7 fluorescence for unconjugated control NP: Cy7-CDEX-0 ($n = 2$), carried out on day 10, 17, 24, and 31 postinjection, expressed as percent of the day 10 emission. The percent remaining after 7 days (day 17) suggests ~5 days half-life, is complicated by transit outward from the center of the vitreous. Less than 1% of the day 10 flux was observed on days 24 and 31, implying a half-life of eye clearance <3 days. Detail of fluxes is shown on Table 3. (**C**) Percent remaining Cy7 fluorescence in time point in vivo IVIS scans of NPCs: Cy7-CDEX-2R ($n = 3$), same time points as above and; Cy7-CDEX-3R ($n = 3$) time points as above with an additional scan at day 52. Half-lives: Cy7-CDEX-2R 7 days; Cy7-CDEX-3R 17 days, based on one phase exponential decay analysis by graphing software (GraphPad Prism version 7; GraphPad Software, La Jolla, CA, USA). Quantitative fluorescence detail is shown on Table 3.

Investigative Ophthalmology & Visual Science

Table 2. IVIS Detected Photons/S as Function of Cy7 (Two Forms) Injected Per Eye

	Cy7-Dex-10	Cy7-Thio-Peptide	Cy7-Dex-10	Cy7-Thio-Peptide	Cy7-Dex-10	Cy7-Dex-10	Cy7-Thio-Peptide
Nanomoles injected per eye	0.06 (0.65 μg)	0.06 (0.13 μg)	0.11 (1.2 μg)	0.12 (0.26 μg)	0.21 (2.3 μg)	0.34 (3.7 μg)	0.46 (5.1 μg)
Detected emission (800 nm)							
Photons ($\times 10^9$)/s	3.8	3.6	6.2	8.5	13.9	25.9*	30.9
Photons ($\times 10^9$)/s per injected nmol	63	60	56	71	66	76	67

Cy7-thio-peptide (2.2 kDa) 50 μL injection ($n = 1$ per dose); Cy7-Dex-10 (11 kDa) 100 μL injection ($n = 2$ per dose).
* One duplicate discarded as outlier.

percentage of CDEX-3R was 65%, the half-life of CDEX-3R was 17 days (range, 10–30 days).

In Vivo Binding Capacity of CDEX-2R Is Exceeded at Doses Above 180 μg per Eye

The above measurements were all in eyes injected with 30 μL of NP or NPCs at 3 mg/mL (90 μg total NP/NPC mass). In order to determine how retention capacity varied with total polymer dose, three different concentrations of the same NPC, CDEX-2R, were compared in IVT loss, especially at day 10, and also later times. We chose the less adherent 2R NPC, for this examination because, when exceeding binding capacity, it would be expected to more rapidly contact cells of the eye surface, thereby amplifying the ability to discern any overload-associated toxicity. IVT injection was 30 μL into each rabbit eye of the Cy7-tagged CDEX-2R from stock solutions of (control: 0 mg/mL [$n = 6$], 3 mg/mL [$n = 3$], 6 mg/mL [$n = 2$], and 12 mg/mL [$n = 2$]). Fluorescence was measured by IVIS as described above, subtracting average autofluorescence from 0 mg/mL (vehicle injection). First scan was 10 days postinjection, and photon flux photon flux shown in Figure 7A at this and subsequent times. The day 10 photons/s values were for 0 mg/mL (0.85×10^9 photons/s -autofluorescence), 3 mg/mL (7.2×10^9 photons/s), 6 mg/mL (16.1×10^9 photons/s), and 12 mg/mL (4.95×10^9 photon/s), the last being a much lower than expected dose-proportional value near $25–30 \times 10^9$ photons/s. Within experimental error, the total fluorescence at day 10 of the eyes receiving injections from 3 mg/mL and 6 mg/mL solutions were proportional to total dose. Eyes receiving high dose (360 μg total) had lower day 10 intensity than even the lowest dose eyes (90 μg), indicating the former exceeded ionic binding capacity of HA in rabbit eyes (1.5–2.0 mL vitreous volume). We attribute this unexpectedly low fluorescence value at the highest dose to excessive load. The loss of residual NPC over 3 weeks after initial day 10 measurement is shown on Figure 7B as a semi-log plot, taking the day 10 emission as "day 0" (100%). The $t_{1/2}$ values at the two lower doses are similar to those observed earlier (7–8 days), while loss or residual emission was surprisingly slower ($t_{1/2}$ near 12 days) for the high dose eyes. All NPC were >95% eliminated from the vitreous after 5 weeks beyond day 10.

Safety Evaluation

Eyes were enucleated immediately after euthanasia, and immediately fixed in 10% buffered formalin. All eyes were examined histologically using standard techniques, and no changes attributable to drug toxicity were seen. No inflammation was observed in any of the ocular tissues in the sections examined. Some changes consistent with injection or mechanical trauma during or postenucleation were noted. Isolated instances of developmental abnormalities in the retina and ciliary body were also observed. These abnormalities were not associated with any dose group.

Discussion

IVT drug delivery systems that achieve longer duration of pharmacologic effect with lower frequency are urgently needed. This has been approached with biodegradable MP, or implantable devices for both small molecules,[24] and for protein anti-VEGF agents.[25] Particle-based delivery of the latter has been reportedly extended for up to 6 months,[26] albeit with movement of visible particulates from the vitreous to the anterior chamber. Observation of foreign body inflammatory responses to IVT-injected, spherical PLGA microspheres in rabbits,[12] with more intense and prolonged such reactions recently seen in nonhuman primates (NHP)[13] drives the search for alternative methods of delivery. Nanotechnology presents opportunities for posterior delivery of drugs and genes, to reduce injection frequency, improve compliance and patient outcome, and includes a variety of devices and materials to enhance access.[27] MP and NP, comprising liposome or micellar structures, have also been utilized, including for gene therapy.[28] Manufacturing lipid NP is problematic because of their high affinity for endotoxin,[29] inserted in their structure, and the finding that tissue contacting vitreous is exceptionally

Table 3. Average of Flux (Photons/s) Detected by IVIS

	Flux, Photons/s ($\times 10^9$)			
Time (Days)	CDEX-0-Cy7, $n = 2$	CDEX-2R-Cy7, $n = 3$	CDEX-3R-Cy7, $n = 2$	Outlier Eye
10	1.6 ± 0.2	6.4 ± 0.28	5.0 ± 0.28	26.3*
17	0.56 ± 0.08	3.2 ± 1.0	4.5 ± 1.5	–
24	0.01 ± 0.01	1.4 ± 0.71	2.9 ± 1.6	10.8*
31	0 ± 0.11	0.97 ± 0.60	1.7 ± 0.22	10.2*
52	–	–	1.3 ± 0.80	7.7*
Half-lives (days, range)	5.1 (3.0–9.4)	6.9 (5.6–8.6)	16.9 (10.3–32.7)	–

Half-lives estimated as described in legends for Figures 6B and 6C. A dash indicates no data.
* 3R-NPC not used for average.

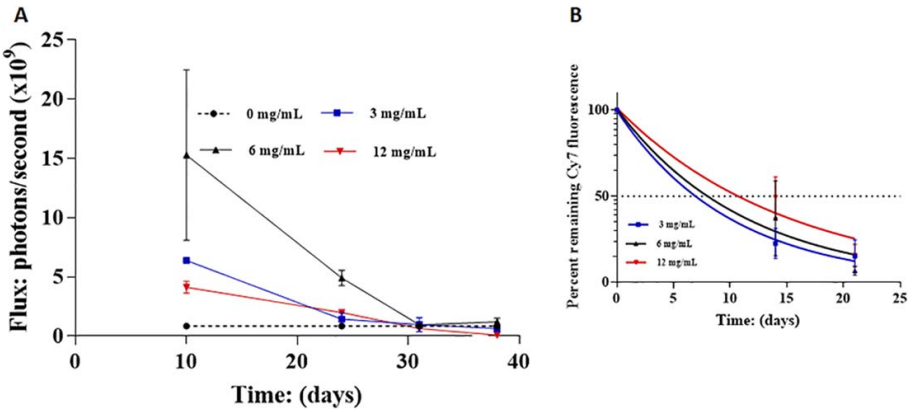

FIGURE 7. Early clearance of IVT injected Cy7-CDEX-2R, at elevated total dose. (**A**) In vivo loss of Cy7-CDEX-2R from rabbit vitreous is shown as photons/s (normalized to cm^2 in 3.5 cm^2 circles) for 3 distinct doses, one being the dose (30 μL at 3 mg/mL, 90 μg total) described in Figure 6C. IVIS scans were taken at day 10, 24, 31, and 38. Cy7-CDEX-2R (30 μL) was from stocks at 4 different concentrations: control, 0 mg/mL ($n = 3$); 3 mg/mL ($n = 3$); 6 mg/mL ($n = 2$); and 12 mg/mL ($n = 2$). Samples at 3 mg/mL and 6 mg/mL (180 μg total) gave proportional day 10 photons/second emission. NPC at 12 mg/mL (360 μg total dose) was much lower at the earliest scan, even below the 4X lower dose. (**B**) Later time points are shown as percent emission remaining compared to day 10 (taken as "day 0", 100%). Half-life of residual NPC loss, after day 10, at the two lower doses, is similar to that observed previously. The residual loss, at the highest dose is slower.

sensitive to endotoxin.[30] Cationic particles, as described here, also attract anionic endotoxin micelles but, without surface lipid, these should be removable by immobilized poly-histidine.[31]

Here we define a sterile-filterable, cationic NP system for sustained IVT residence, where diameter <100 nm makes foreign body response unlikely. The long wavelength fluorophore, Cy7, used here, has been employed to track bone-targeted NP in mice,[32] with common IVIS instrumentation, and has recently been applied to monitor NP distribution in isolated rabbit hearts after intracardiac injection in a similar IVIS chamber.[33] Rabbit eye closely models human eye PK over a wide range of agents,[7] and the present study tracks Cy7-NP/NPC to estimate their eye clearance in small rabbits, under brief anesthesia.

Consistent with our previous rodent results[17] we showed (Fig. 4) that rapid NP clearance in rabbit eyes was slowed in NPC conjugated with 2R-peptides. This was further slowed by similar loading with 3R-peptides, diffusion being inversely related to positive zeta potential, with >20% of tagged 3R-NPC apparently present 6 weeks after first scan of an IVT injection (Fig. 5). The in vivo quantitative IVIS analysis was validated by relating emitted photons to ex vivo IVT injections of varied, smaller Cy7 compounds in enucleated rabbit eyes, showing these were proportional over the relevant range, justifying quantitation by IVIS in live rabbit eyes, of IVT NPC loss (Fig. 6A; Table 2). Our rodent study is here extended to in vivo monitoring of larger eyes, estimated over 10 to 52 days after IVT injection. We related the half-life of IVT residence to zeta potentials (range: +3.9 to +6.3 mV), results suggesting that $t_{1/2}$ of 1 to 3 weeks is attainable with 2R and 3R-peptide conjugates, carrying 60 peptides/NPC. It is likely that 4R peptides, available in, say 5 to 8 amino acid fragments of protamine 1, can be attached at similar loading, and will display longer $t_{1/2}$, targeting zeta potential in the range of +10 to +15 mV. NPC of 4R-peptides should be explored, expecting IVT half-life, at or above 6 weeks, based on our previous observations.[17]

While only describing a clearance rate range, with large error bars, limited by the small number of injected eyes in this pilot study, our ex vivo analysis (Fig. 6A; Table 2) indicates that a Cy7 tag gives intraocular, concentration-dependent 800 nm IVIS emission, in vivo, with variability no greater than might be expected for natural variation in volume and poly-anion composition among rabbit eyes. Although $t_{1/2}$ values reported here are semiquantitative estimates, our described method should enable significant PK comparisons when greater numbers are available. Our most significant source of variability arises in that NP and NPC, though sterile-filtered, remain a polydisperse conjugate mixture. While beyond the scope of this preliminary evaluation, it will be essential, in future work to apply gel-filtration to improve NP/NPC monodispersity.

The carriers used have two types of site to contain drug cargo, a hydrophobic core for small lipophilic agents, and OH groups for prodrug metastable linking at the surface.

Our observation that 2R-NPC exceeded vitreal binding capacity when total injection in 1.5 to 2 mL rabbit vitreous exceeded 180 μg, suggests that a human vitreous of about 4 mL might be effectively limited to 400 μg, or somewhat higher with more tightly bound 3R or 4R-NPC, if human vitreal HA is higher than that of rabbit, as has been proposed.[34] Thus, lipophilic small molecule cargo, contained in the cholesteryl core may be in the range of 10 to 100 μg. Agents such as brimonidine, sirolimus, doxorubicin, or taxanes might well be contained, but their rate of exit to free solution requires kinetic examination. Surprisingly, with the highest dose, subsequent loss of residual NPC displayed $t_{1/2}$ of 12 days while that of the two lower doses was near 7 days (Fig. 7B). We speculate that slower NPC loss, following the rapid early loss, is due to a more highly cationic NPC subpopulation remaining bound when capacity is initially exceeded.

The NPC surface has capacity to carry esters of carboxyl-containing agents. We have found that spontaneous hydrolysis half-lives of such carboxylic drug esters can be modulated to range from 20 to 90 days with amino-alcohol bridging (data not shown, manuscript in preparation). Thus, diclofenac and methotrexate could be delivered as direct or amine-bridged esters.

Utilizing adherence to intravitreal HA has also been recently employed, attempting to prolong the IVT residence of anti-VEGF proteins. Fusions between one such Fab fragment and a 97-amino-acid LINK domain of a hyaladherin protein gave 30-fold higher IVT Fab fusion protein at 30 days, compared with Ranibizumab at 21 days.[34] However, this introduces a novel epitope at the fusion site.

Anti-VEGF proteins can likely be attached at 1–2 mol per NPC, where >200 μg cargo per eye is a potential target. These

may be attached via disulfide bonds with cysteine peptides, where intraocular glutathione drives release, or via esters bridging protein-SH and appended NPC cysteines through bifunctional linkers. An anti-VEGF protein ($t_{1/2}$ 6 days) injected at 1 mg/eye could well diminish, by first order decay, to <1 μg at 60 days. If NPC, with 200 μg linked protein, is given, and has 42-day residence $t_{1/2}$, where hydrolytic release also has $t_{1/2}$ of 42 days, significant concentrations of active free protein, may be sustained through the 8 to 12-week period postinjection. As suggested previously,[34,35] the rabbit IVT HA binding capacity for our NPC may significantly underestimate that of human eyes. IVT HA has been found to be near 270 μg/mL in nonrhegmatogenous vitrectomy patients,[36] while it is reported below 50 μg/mL in rabbits.[37] Thus, a 1-mg clinical load of 3R-NPC may well be within human IVT capacity, with a comparable amount of linked anti-VEGF, enabling release >4 to 5 μg daily at 80 to 90 days postinjection, a significant extension of IVT concentration for active protein agents.

Conclusions

Polycationic NPC, comprising condensed dextran and small, appended L-Arg peptides, can safely maintain prolonged IVT residence, with $t_{1/2}$ in a 1- to 3-week range, with doses up to 100 μg/mL vitreous. Usefulness will depend on individual drug potency and release rate, superimposed on extended IVT presence. While these NPC appear nontoxic to the rabbit eye, a more definitive study to completely rule out significant drug toxicity, is needed before human administration. Therapeutic use will require extensive histology, also tests of ERG and intraocular pressure in other species, including NHP.

Acknowledgments

Supported by an unrestricted award from Research to Prevent Blindness to the Department of Ophthalmology and Visual Sciences, Retina Research Foundation, P30 EY016665, P30 CA014520, EPA 83573701, R24 EY022883, and R01 EY026078. CMS is supported by the RRF/Daniel M. Albert Chair. NS is a recipient of RPB Stein Innovation Award. Peptides were synthesized by the Peptide Synthesis Core and NP/NPC size and ζ were measured by the Analytical BioNanoTechnology Equipment Core (ANTEC) of Simpson Querrey Institute (SQI) at Northwestern University (NU; Chicago, IL, USA). Also supplied by Erin and Wellington Hsu of SQI were enucleated rabbit eyes for IVIS study. IVIS studies used facilities of the Center for Advanced Molecular Imaging (CAMI), Evanston, Illinois, United States. Charlette M. Caine, DVM, NU, contributed assistance and training in enucleation of euthanized rabbit eyes.

Disclosure: **I. Melgar-Asensio**, P; **I. Kandela**, None; **F. Aird**, None; **S.R. Darjatmoko**, None; **C. de los Rios**, None; **C.M. Sorenson**, None; **D.M. Albert**, None; **N. Sheibani**, None; **J. Henkin**, P

References

1. Jonasson F, Fisher DE, Eiriksdottir G, et al. Five-year incidence, progression, and risk factors for age-related macular degeneration: the age, gene/environment susceptibility study. *Ophthalmology*. 2014;121:1766–1772.
2. Willis JR, Doan QV, Gleeson M, et al. Vision-related functional burden of diabetic retinopathy across severity levels in the United States. *JAMA Ophthalmol*. 2017;135:926–932.
3. Booth BA, Kang-Mieler JJ, Osswald CR, Mieler WF. Advances in ocular drug delivery: emphasis on the posterior segment. *Expert Opin Drug Deliv*. 2014;11:1647–1660.
4. Tan HY, Agarwal A, Lee CS, et al. Management of noninfectious posterior uveitis with intravitreal drug therapy. *Clinical Ophthalmol*. 2016;10:1983–2020.
5. Ghate D, Edelhauser HF. Barriers to glaucoma drug delivery. *J Glaucoma*. 2008;17:147–156.
6. Shen J, Durairaj C, Lin T, Liu Y, Burke J. Ocular pharmacokinetics of intravitreally administered brimonidine and dexamethasone in animal models with and without blood-retinal barrier breakdown. *Invest Ophthalmol Vis Sci*. 2014;55:1056–1066.
7. del Amo EM, Vellonen KS, Kidron H, Urtti A. Intravitreal clearance and volume of distribution of compounds in rabbits: In silico prediction and pharmacokinetic simulations for drug development. *Eur J Pharm Biopharm*. 2015;95:215–226.
8. Moisseiev E, Waisbourd M, Ben-Artsi E, et al. Pharmacokinetics of bevacizumab after topical and intravitreal administration in human eyes. *Graefes Arch Clin Exp Ophthalmol*. 2014;252:331–337.
9. Falavarjani KG, Nguyen QD. Adverse events and complications associated with intravitreal injection of anti-VEGF agents: A review of literature. *Eye (Lond)*. 2013;27:787–794.
10. del Amo EM, Rimpelä AK, Heikkinen E, et al. Pharmacokinetic aspects of retinal drug delivery. *Prog Retin Eye Res*. 2017;57:134–185.
11. Peeters L, Sanders NN, Braeckmans K, et al. Vitreous: a barrier to nonviral ocular gene therapy. *Invest Ophthalmol Vis Sci*. 2005;46:3553–3561.
12. Giordano GG, Chevez-Barrios, P, Refoio MF, Garcia CA. Biodegradation and tissue reaction to intravitreous biodegradable poly (D, L-lactic-co-glycolic) acid microspheres. *Curr Eye Res*. 1995;14:761–768.
13. Thackaberry EA, Farman C, Zhong F, et al. Evaluation of the toxicity of intravitreally injected PLGA microspheres and rods in monkeys and rabbits: effects of depot size on inflammatory response. *Invest Ophthalmol Vis Sci*. 2017;58:4274–4285.
14. Kim H, Robinson SB, Csaky KG. Investigating the movement of intravitreal human serum albumin nanoparticles in the vitreous and retina. *Pharm Res*. 2009;26:329–337.
15. Xu QG, Boylan NJ, Suk JS, et al. Nanoparticle diffusion in, and microrheology of, the bovine vitreous ex vivo. *J Control Release*. 2013;167:76–84.
16. Zern BJ, Chu H, Osunkoya AO, Gao J, Wang Y. A biocompatible arginine-based polycation. *Adv Funct Mater*. 2011;21:434–440.
17. Li H, Liu W, Sorenson CM, et al. Sustaining intravitreal residence with L-Arginine peptide-conjugated nanocarriers. *Invest Ophthalmol Vis Sci*. 2017;58:5142–5150.
18. Lumiprobe. Cyanin7 Amine. Available at: https://www.lumiprobe.com/p/cy7-amine.
19. Bernard A, Gao-Li J, Franco C-A, Bouceba T, Huet A, Zhenlin L. Laminin receptor involvement in the anti-angiogenic activity of pigment epithelium-derived factor. *J Biol. Chem*. 2009;284:10480–10490.
20. Bagnéris C, Bateman OA, Naylor CE, et al. Crystal structures of alpha-crystallin domain dimers of alpha B-crystallin and Hsp20. *J Mol Biol*. 2009;392:1242–1252.
21. Chiu H-C, Koňák C, Kopecková P, Kopecek J. Enzymatic degradation of poly-(ethylene glycol) modified dextrans. *J Bioact Compat Polym*. 1994;9:388–410.
22. Vandoorne F, Vercauteren R, Permentier D, Schacht E. Reinvestigation of the 4-nitro-phenyl chloroformate activation of dextran. Evidence for the formation of different types of carbonate moieties. *Makromol Chem*. 1985;186:2455–2460.

23. Ramirez JC, Sanchez-Chaves M, Arranz F. Dextran functionalized by 4-nitrophenyl carbonate groups. *Die Angewandte Makromolekulare Chemie*. 1995;225:123–130.
24. Lance KD, Good SD, Mendes TS, et al. In vitro and in vivo sustained zero-order delivery of rapamycin (sirolimus) from a biodegradable intraocular device. *Invest Ophthalmol Vis Sci*. 2015;56:7331–7337.
25. Kuno N, Fujii S. Biodegradable intraocular therapies for retinal disorders: progress to date. *Drugs Aging*. 2010;27:117–134.
26. Adamson P, Wilde T, Dobrzynski E, et al. Single ocular injection of a sustained-release *anti*-VEGF delivers 6 months pharmacokinetics and efficacy in a primate laser CNV model. *J Control Release*. 2016;244(part A):1–13.
27. Kompella UB, Amrite AC, Ravia RP, Durazo SA. Nanomedicines for back of the eye drug delivery, gene delivery, and imaging. *Prog Retin Eye Res*. 2013;36:172–198.
28. Wang Y, Rajala A, Raju V, Rajala RVS. Lipid nanoparticles for ocular gene delivery. *J Funct Biomater*. 2015;6:379–394.
29. Magalhães PO, Lopes AM, Mazzola PG, Rangel-Yagui C, Penna TCV, Pessoa A Jr. Methods of endotoxin removal from biological preparations: a review. *J Pharm Pharmaceut Sci*. 2007;10:388–404.
30. Bantseev V, Miller PE, Bentley E, et al. Determination of a no-observable effect level for endotoxin following a single intravitreal administration to Dutch belted rabbits. *Invest Ophthalmol Vis Sci*. 2017;58:1545–1552.
31. Bosshart H, Heinzelmann M. Arginine-Rich cationic polypeptides amplify lipopolysaccharide-induced monocyte activation. *Infect Immun*. 2002;70:6904–6910.
32. Rudnick-Glick S, Corem-Salkmon E, Grinberg I, Yehuda R, Margel S. Near IR fluorescent conjugated poly (ethylene glycol) bisphosphonate nanoparticles for in vivo bone targeting in a young mouse model. *J Nanobiotechnol*. 2015;13:80–87.
33. Segura-Ibarra V, Cara FE, Wu S. Nanoparticles administered intrapericardially enhance payload myocardial distribution and retention. *J Control Release*. 2017;262:18–27.
34. Ghosh JG, Nguyen AA, Bigelow CE, et al. Long-acting protein drugs for the treatment of ocular diseases. *Nat Commun*. 2017;8:14837.
35. Coulson-Thomas VJ, Lauer ME, Soleman S, et al. Tumor necrosis factor stimulated gene-6 (TSG-6) is constitutively expressed in adult central nervous system (CNS) and associated with astrocyte-mediated glial scar formation following spinal cord injury. *J Biol Chem*. 2016;291:19939–19952.
36. Kaprinis K, Symeonidis C, Papakonstantinou E, Ioannis Tsinopoulos I, Dimitrakos A. Decreased hyaluronan concentration during primary rhegmatogenous retinal detachment. *Eur J Ophthalmol*. 2016;26:633–638.
37. Necas J, Bartosikova L, Brauner P, Kolar J. Hyaluronic acid (hyaluronan): a review. *Veterinarni Medicina*. 2008;53:397–411.

Investigative Ophthalmology & Visual Science